

Coupling a water balance model with forest inventory data to predict drought stress: the role of forest structural changes vs. climate changes



Miquel De Cáceres ^{a,b,*}, Jordi Martínez-Vilalta ^{b,c}, Lluís Coll ^{a,b}, Pilar Llorens ^d, Pere Casals ^a, Rafael Poyatos ^b, Juli G. Pausas ^e, Lluís Brotons ^{a,b,f}

^a InForest Joint Research Unit, CTFC-CEMFOR, Solsona25280, Spain

^b CREAf, Cerdanyola del Vallès 08193, Spain

^c Universitat Autònoma de Barcelona, Cerdanyola del Vallès 08193, Spain

^d Institute of Environmental Assessment and Water Research (IDAEA-CSIC), Barcelona 08034, Spain

^e Centro de Investigaciones sobre Desertificación (CIDE-CSIC), Valencia, Spain

^f CSIC, Cerdanyola del Vallès 08193, Spain

ARTICLE INFO

Article history:

Received 3 December 2014

Received in revised form 4 May 2015

Accepted 21 June 2015

Keywords:

Drought stress

Forest inventory data

Mediterranean forests

Water balance model

ABSTRACT

Mechanistic water balance models can be used to predict soil moisture dynamics and drought stress in individual forest stands. Predicting current and future levels of plant drought stress is important not only at the local scale, but also at larger, landscape to regional, scales, because these are the management scales at which adaptation and mitigation strategies are implemented. To obtain reliable predictions of soil moisture and plant drought stress over large extents, water balance models need to be complemented with detailed information about the spatial variation of vegetation and soil attributes. We designed, calibrated and validated a water balance model that produces annual estimates of drought intensity and duration for all plant cohorts in a forest stand. Taking Catalonia (NE Spain) as a case study, we coupled this model with plot records from two Spanish forest inventories in which species identity, diameter and height of plant cohorts were available. Leaf area index of each plant cohort was estimated from basal area using species-specific relationships. Vertical root distribution for each species in each forest plot was estimated by determining the distribution that maximized transpiration in the model, given average climatic conditions, soil attributes and stand density. We determined recent trends (period 1980–2010) in drought stress for the main tree species in Catalonia; where forest growth and densification occurs in many areas as a result of rural abandonment and decrease of forest management. Regional increases in drought stress were detected for most tree species, although we found high variation in stress changes among individual forest plots. Moreover, predicted trends in tree drought stress were mainly due to changes in leaf area occurred between the two forest inventories rather than to climatic trends. We conclude that forest structure needs to be explicitly considered in assessments of plant drought stress patterns and trends over large geographic areas, and that forest inventories are useful sources of data provided that reasonably good estimates of soil attributes and root distribution are available. Our approach coupled with recent improvements in forest survey technologies may allow obtaining spatially continuous and precise assessments of drought stress. Further efforts are needed to calibrate drought-related demographic processes before water balance and drought stress estimates can be fully used for the accurate prediction of drought impacts.

© 2015 Elsevier B.V. All rights reserved.

1. Introduction

Drought stress is a key factor to understand the dynamics of most terrestrial ecosystems worldwide. Although drought impacts are often progressive and cumulative, reports of large-scale events of drought-related forest decline are increasingly common and have been linked to on-going global warming (Allen et al., 2010;

Abbreviations: DDS, daily drought stress; DI, drought intensity; NDD, number of drought days; LAI, leaf area index; PET, potential evapotranspiration; SFI, spanish forest inventory.

* Corresponding author at: Centre Tecnològic Forestal de Catalunya. Ctra. antigua St. Llorenç km 2, E-25280-Solsona, Catalonia, Spain. Fax: +34 973 48 13 92.

E-mail address: miquelcaceres@gmail.com (M.D. Cáceres).

Carnicer et al., 2011). Being able to anticipate where, when and which plant species will be impacted by cumulative drought or extreme drought events is particularly important at landscape to regional scales, because strategies focusing on adaptation and mitigation of drought impacts are normally designed and implemented at these scales (e.g., Lindner et al., 2010).

Assessments of plant drought stress can be obtained using a range of approaches differing in the drought definition, the spatial and temporal resolution, the degree of complexity and the amount of information required (Dai, 2011; Heim, 2002). While meteorological drought is routinely quantified using indices that employ temperature and precipitation data obtained from ground meteorological stations (e.g., McKee et al., 1993; Palmer, 1965; Vicente-Serrano et al., 2010), soil moisture, vegetation stress and decline are usually monitored for large areas using indices derived from satellite remote sensing (e.g., Deshayes et al., 2006; Gao, 1996; Gobron et al., 2006; Kerr et al., 2012; Kogan, 1997). An alternative, or complementary, way of estimating drought stress is by using process-based models that, given some meteorological, edaphic and vegetation data, are able to predict temporal variations of soil moisture and plant drought stress (e.g., Granier et al., 2007; Lafont et al., 2012; Ruffault et al., 2013). Compared to drought monitored by remote sensing, process-based models have the advantage of allowing drought stress to be explicitly differentiated from other factors affecting plant health condition, such as pests, diseases or air pollution (Deshayes et al., 2006). Moreover, they allow future drought stress impacts to be anticipated when coupled with climatic projections (e.g., Ruffault et al., 2014).

Different kinds of process-based models (e.g., hydrological models, ecosystem models, forest gap models, landscape dynamics models or dynamic global vegetation models) include modules to calculate soil water balance (e.g., Bugmann and Cramer 1998; Davi et al., 2005; Dufrêne et al., 2005; Lischke et al., 2006; Martínez-Vilalta et al., 2002; Mouillot et al., 2001; Running and Coughlan, 1988; Sitch et al., 2003; Sus et al., 2014) and, hence, can be used to track temporal variation in drought stress. These models often differ in spatial resolution and the amount of detail of the representation of soil and vegetation. They also differ in the representation of processes related to water fluxes and drought stress (i.e., meteorological, hydrological, physiological or demographic processes).

Although many process-based models include more or less detailed soil water balance calculations, not all models are equally suited to obtain species-specific maps showing drought stress over entire landscapes or regions. Since plant species differ in their strategy to cope with drought and their ability to extract water at different soil water potentials, the design of the chosen model should be able to simulate the competition of plant cohorts and species for local water resources (e.g., Mouillot et al., 2001). Moreover, the definition of state variables should include leaf area, or a close surrogate, because the leaf area of a stand strongly influences soil moisture dynamics and, in turn, the intensity and duration of drought stress (e.g., Joffre and Rambal, 1993). Finally, the application of a model with very detailed representation of processes may be constrained for landscape and regional applications by the high number of parameters required. Such extensive applications are better approached using a simpler but robust model easy to parameterize for a broad range of environmental conditions (Ruffault et al., 2014, 2013).

Assessing plant drought stress over landscapes and regions using process-based models requires detailed spatial information of soil and vegetation attributes. While not spatially continuous, the systematic sampling and repeated surveys of national forest inventories allow the forest structure and composition to be monitored for large geographic areas. Data from forest inventories have already been used in combination with ecosystem models to predict primary production and water and carbon fluxes over

landscapes and regions (e.g., Keenan et al., 2011; Le Maire et al., 2005). However, the design of the models employed in these exercises did not allow distinguishing the drought stress of cohorts and species coexisting in forest plots. This level of detail in drought stress assessments is important, for example, for assisting management decisions aimed to improve the resilience of forests in front of drought impacts. Moreover, species-specific drought stress assessments are a key component of landscape simulation models aimed at anticipating the effects of drought in combination with other drivers such as wildfires or insect outbreaks (e.g., Fyllas and Troumbis, 2009; Gustafson and Sturtevant, 2013).

In this paper we explore the potential advantages and limitations of coupling forest inventory data with a water balance model to monitor the amount of drought stress experienced by plant species over large areas. We first present the design, parameterization and validation of a water balance model that allows tracking soil moisture variations and quantifying drought stress for plant cohorts (of the same or different species) in forest stands. The state base of the model is adapted for its use in combination with forest inventory data, whereas the complexity in terms of processes is kept very simple to reduce the number of parameters and facilitate its application to different areas. We use Catalonia (NE Spain) as a case study and take the Second and Third Spanish National Forest Inventories in that region as source of vegetation structure and composition data for the water balance model. After estimating leaf area indices and vertical root distribution for each plant cohort in each forest plot, we examine two other issues that may compromise the use of this approach. First, we ask to what extent incomplete knowledge regarding soil depth may preclude obtaining accurate predictions of drought stress. Second, by comparing the predictions obtained using the two forest inventories, we determine to what extent local and regional-average drought stress assessments may be biased when conducted several years after a given survey. Finally, we illustrate our approach by determining recent temporal trends (1980–2010) in drought stress for the main tree species in the study area. Our hypothesis in this application is that vegetation changes occurred during this period should explain an important part of the variability in drought stress. Hence, we distinguish between the effect of climatic variations and the effect of changes in vegetation structure.

2. Materials and methods

2.1. Water balance model and drought stress definition

The purpose of the water balance model is to predict temporal variations in soil water content and assess drought stress for plants in a forest stand. Our model follows the design principles of BILJOU (Granier et al., 1999; Granier et al., 1999) and SIERRA (Mouillot et al., 2001; Ruffault et al., 2014, 2013), with some characteristics taken from dynamic global vegetation models (Prentice et al., 1993). The model calculates water balance on a daily basis. Soil is represented using two layers – topsoil and subsoil – and the model keeps track of the proportion of moisture relative to field capacity for each layer. Soil water holding capacity includes the effects of rock fragment content. Vegetation is represented as a set of plant cohorts having different height, root distribution, species identity and leaf area index (LAI; i.e., the one-side area of leaves corresponding to the cohort per unit of stand surface area). The root system of each cohort is described by the vertical distribution of its fine root biomass, calculated following the linear dose response model (Schenk and Jackson, 2002) (see Section 2.6 and Appendix S1). The minor fraction of root mass located below soil depth is redistributed within the existing layers and the proportion of fine roots in each soil layer is assumed proportional to the amount of water extracted from it.

Every day the model first updates leaf area of (semi-) deciduous plants according to a simple phenological model that determines leaf budburst and leaf fall, where parameter S_{GDD} indicates the growth degree days necessary for budburst (evergreen plants are assumed to have constant leaf area throughout the simulation). Then, the model recalculates light extinction through the canopy, following the Beer-Lambert model, and the water storage capacity of the canopy (i.e., the minimum amount of water needed to saturate the canopy). Species-specific parameters needed for these calculations are the light extinction coefficient (k_{sp}), the bole height proportion (b_{sp}) and the canopy water storage capacity per LAI unit (s_{sp}). After updating the canopy status, the model deals with the water input from rainfall. Before increasing the water content of soil layers, the model first subtracts the water lost due to interception and the water lost through surface runoff from rainfall. Rainfall interception loss is estimated using the sparse version of the Gash model (Gash et al., 1995) and runoff is estimated using the USDA SCS curve number method according to Boughton (1989). Lateral water transfer processes are not considered. Soil water storage capacity and water potential are calculated from texture using pedotransfer functions (Saxton et al., 1986). When refilling a given soil layer, a proportion of water is assumed to directly percolate to the next layer below, as dictated by macroporosity (Granier et al., 1999). The water percolating from the deepest layer is assumed to be lost via deep drainage.

After refilling soil layers, the model determines evapotranspiration losses. Daily potential evapotranspiration (PET) is determined following the theory of equilibrium evapotranspiration (Jarvis and McNaughton, 1986; Prentice et al., 1993). Evaporation from the soil surface is controlled by PET, the amount of light reaching the ground and the water content of the topsoil, but the reduction in moisture is divided among the two soil layers according to a negative exponential function (Ritchie, 1972). To determine plant transpiration, the model first determines the maximum transpiration of the whole stand (i.e., assuming that water is not limiting) as a function of the stand's LAI and PET (Granier et al., 1999). Following Mouillot et al. (2001), the amount of water extracted by a plant cohort from a given soil layer is defined as the product of: (i) the maximum transpiration of the stand; (ii) the proportion of maximum transpiration that corresponds to the plant cohort, calculated on the basis of its leaf area and the amount of light available to it; (iii) the relative whole-plant conductance corresponding to the water potential in the soil layer; (iv) the proportion of fine roots in the soil layer. Relative whole-plant conductance lies between 0% (no conductance) and 100% (maximum conductance) and depends on the water potential in the soil layer and Ψ_{sp} , the species-specific water potential corresponding to 50% loss of conductance. Ψ_{sp} is a model parameter that integrates all the processes that may affect whole-plant water conductance, including stomatal regulation, xylem embolism and changes at the soil-root interface (Sperry et al., 1998; Martínez-Vilalta et al., 2014). Therefore, its interpretation may differ depending on the behavior of the species under drought (e.g., McDowell et al., 2008). For relatively isohydric species Ψ_{sp} would mostly reflect the soil water potential associated to stomata closure, whereas for relatively anisohydric species Ψ_{sp} may be controlled by their vulnerability to xylem embolism.

Granier et al. (1999) and Granier et al. (2007) defined drought stress to begin when soil relative extractable water was below 40%, whereas in Ruffault et al. (2014, 2013), drought periods start when soil water potential drops below -0.5 MPa (a value beyond which a decrease in canopy conductance is observed for many Mediterranean species; Limousin et al., 2009). Following Mouillot et al. (2002), we defined drought stress periods for a given plant cohort as periods when relative whole-plant conductance is below 50%. Daily drought stress (DDS) of a plant cohort is defined as the

one-complement of the relative conductance integrated across soil layers (Collins and Bras, 2007):

$$\text{DDS}_i = \varphi_i \times \sum_s (1 - K_{i,s}) \times v_{i,s} \quad (1)$$

where $K_{i,s}$ is the relative whole-plant conductance of cohort i in layer s ; $v_{i,s}$ is the proportion of the fine roots that cohort i has in layer s ; and φ_i is the cohort leaf-phenological status ($\varphi_i \in [0,1]$), included to avoid winter deciduous plants from suffering drought stress during winter. We quantified annual drought duration as the number of drought days (NDD) with relative conductance below 50% (i.e., DDS > 0.5) and annual drought intensity (DI) as:

$$\text{DI} = \frac{\sum_s \max[(0.5 - \text{DDS})/0.5, 0]}{365} \quad (2)$$

where DI is dimensionless and ranges between 0 (relative conductance always > 50%) and 1 (0% relative conductance during all year).

Additional details of the design and specific formulation of the water balance model are given in Appendix S1. Predicted drought intensity and duration are strongly sensitive to changes in annual rainfall and leaf area index, but other parameters like soil depth and root distribution also appear to be influential (see sensitivity analyses in Appendix S2). The model is implemented in C++ and is executed from an interface written in R language. An R package is available upon request to M. De Cáceres.

2.2. Study area and calibration of species-specific parameters

Catalonia (31,144 km²; northeast of Spain; Fig. 1) is a region with 60% of its surface covered by forests and shrublands. Prevailing climate in most of the region is Mediterranean, but strong climatic gradients occur as a result of complex relief and distance to the coast. Mean annual temperature ranges between -0.1 and +17 °C (average +12.3 °C) and annual rainfall ranges between 344 and 1587 mm (average 684 mm). In most of the region, rainfall peaks in autumn and spring (average 222 and 194 mm, respectively), and it is relatively low during summer and winter (average 173 and 141 mm, respectively) (source: Ninyerola et al., 2000). In addition to the characteristic summer water deficit, Mediterranean climate often includes a strong inter-annual variation in rainfall and temperature regimes, which adds uncertainty to the intensity and duration of drought stress.

We treated the 12 most frequent tree species in the study area as separate entities (see Table 1). Less frequent tree species were lumped together in a group named 'other trees' and shrubs were divided into three functional groups related to post-fire regeneration strategies (Keeley et al., 2012): 'Shrub R+S-' (resprouters), 'Shrub R-S+' (seeders) and 'Shrub R+S+' (facultative seeders). The full list of species included in each group is given in Appendix S3. The proportion of bole height (b_{sp}) and light extinction coefficients (k_{sp}) for tree and shrub species were inferred from bibliographic sources (Aubin et al., 2000; Bréda, 2003) (Table 1). To determine soil water potentials related to 50% of water conductance loss, species were divided between strongly isohydric ($\Psi_{sp} = -2.0$ MPa; conifers, beech and 'other trees'), moderately isohydric ($\Psi_{sp} = -3.0$ MPa; oaks and 'shrubs R+S+'), moderately anisohydric ($\Psi_{sp} = -4.0$ MPa; 'shrubs R+S-') and strongly anisohydric ($\Psi_{sp} = -5.0$ MPa; 'shrubs R-S+'). Considering the relatively high uncertainty in the Ψ_{sp} reflecting in part methodological issues (e.g., Delzon and Cochard, 2014), we decided to group species in 'functional types' to avoid generating artificial variability among species and focusing on the differences that are robust enough to be interpretable. The Ψ_{sp} values were established after examining and comparing several bibliographic sources: (1) minimum recorded leaf water potentials for these species (Choat et al., 2012; Martínez-Vilalta et al.,

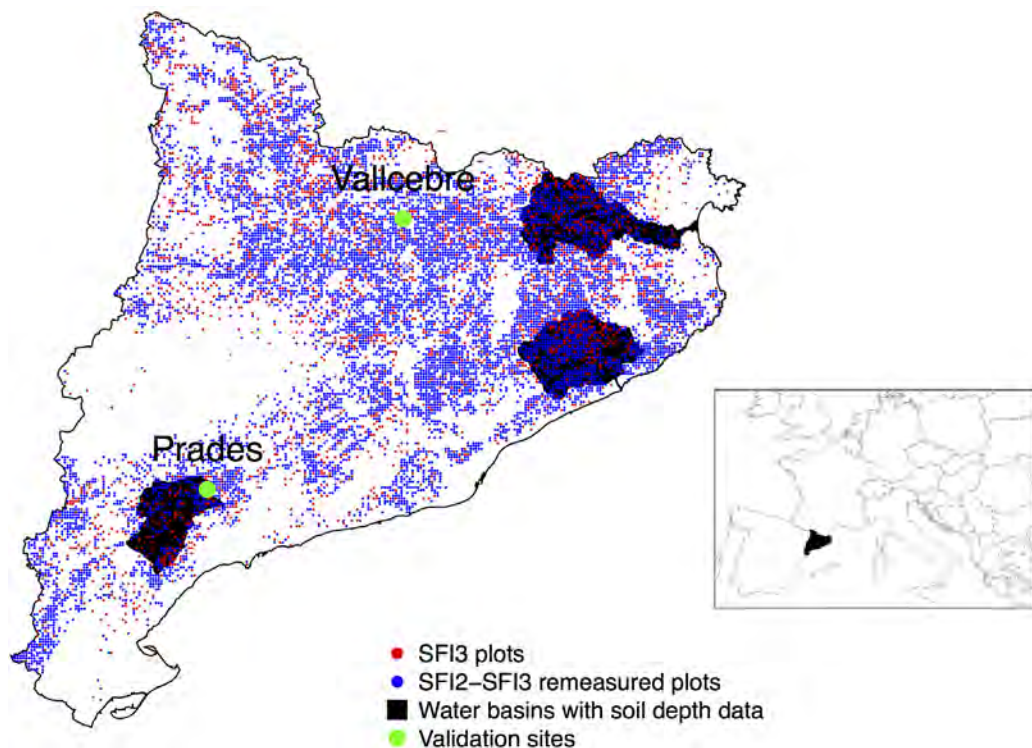


Fig. 1. Location of validation sites and forest inventory plots within Catalonia.

2014); (2) water potentials causing 50% xylem embolism in stems (Choat et al., 2012); (3) water potentials at turgor loss point (Bartlett et al., 2012); and (4) water potentials at 50% stomatal closure (Klein, 2014). Values for s_{sp} , the amount of water that can be retained in the canopy of a particular species per LAI unit, were set after inspecting values reported in experimental studies. Additional information regarding the calibration of s_{sp} and Ψ_{sp} is included in Appendix S3.

2.3. Model evaluation

We evaluated the predictive accuracy of the model with respect to variations in transpiration and soil water content using data from two distinct sites (Fig. 1). *Prades* site is characterized by a Mediterranean climate and has rocky and shallow soils. A process of drought-induced decline of *Pinus sylvestris* is occurring in this site

since the 1990s (Martínez-Vilalta and Piñol, 2002; Poyatos et al., 2013). *Vallcebre* site has a sub-Mediterranean climate and soils are deeper and with lower gravel content (Poyatos et al., 2005; García-Estrada et al., 2013). We gathered soil and vegetation data for one stand in each site (Table 2). Soil attributes were determined from soil samples. As vegetation in *Prades* has been found to rely on deep water reserves during dry periods (Barbeta et al., 2014), we considered both the stand's measured soil depth (40 cm) as well as two additional parameterizations where soil field capacity was increased to account for the additional water volume potentially accessible through rock fissures and cracks (see Table 2). Tree leaf area for each species in each stand was calculated as a function of site-specific allometric relationships between stem/branch diameter and leaf mass/area. Root distribution was estimated by determining the parameters of the linear dose response function

Table 1
 Species-specific model parameters and linear regressions used to estimate LAI. k_{sp} – Extinction coefficient, corresponding to global radiation in the case of trees (Bréda, 2003) and photosynthetic active radiation in the case of shrubs (Aubin et al., 2000); b_{sp} – bole height in relation to total height; s_{sp} – Canopy water storage capacity per LAI unit; Ψ_{sp} – Water potential associated to 50% conductance loss; S_{GDD} – Growth degree days ($T_{base} = 5^\circ\text{C}$) to attain full LAI. LAI-BA – estimated slope of the linear regression between basal area and LAI; n – number of observations; Range – range of basal area values considered; $R^2\text{adj}$ – adjusted R^2 -square.

Species/functional group	k_{sp}	$b_{sp}(\%)$	$s_{sp}(\text{mm LAI}^{-1})$	$\Psi_{sp}(\text{MPa})$	S_{GDD}	LAI-BA	n	BA range(m^2/ha)	$R^2\text{adj}$
<i>Pinus halepensis</i>	0.50	66	1.00	-2.0	–	0.05201	2712	[0.06, 51.39]	93.4%
<i>Pinus nigra</i>	0.50	66	1.00	-2.0	–	0.06626	2063	[0.04, 67.82]	83.5%
<i>Pinus sylvestris</i>	0.50	66	1.00	-2.0	–	0.05213	3211	[0.04, 87.39]	94.2%
<i>Pinus uncinata</i>	0.50	66	1.00	-2.0	–	0.05061	787	[0.05, 82.15]	82.4%
<i>Pinus pinea</i>	0.50	66	1.00	-2.0	–	0.06293	985	[0.05, 48.2]	92.0%
<i>Pinus pinaster</i>	0.50	66	1.00	-2.0	–	0.05095	296	[0.06, 75.6]	82.9%
<i>Abies alba</i>	0.35	30	1.00	-2.0	–	0.10715	230	[0.3, 86.66]	95.3%
<i>Quercus ilex</i>	0.55	50	0.50	-3.0	–	0.14220	4063	[0.02, 56.68]	91.4%
<i>Quercus suber</i>	0.55	50	0.50	-3.0	–	0.03974	1032	[0.08, 62.28]	85.2%
<i>Quercus humilis</i>	0.55	50	0.50	-3.0	200	0.12481	1847	[0.03, 42.65]	91.4%
<i>Quercus faginea</i>	0.55	50	0.50	-3.0	200	0.14989	355	[0.04, 20.74]	72.2%
<i>Fagus sylvatica</i>	0.43	50	0.25	-2.0	200	0.12343	567	[0.07, 72.03]	83.3%
Other trees	0.43	50	0.25	-2.0	200	0.29178	180	[0.07, 14.86]	85.3%
Shrub R+S-	0.40	10	0.25	-4.0	–	0.19319	546	[0.03, 20.00]	92.2%
Shrub R+S-	0.40	10	0.25	-5.0	–	–	–	–	–
Shrub R+S-	0.40	10	0.25	-3.0	–	–	–	–	–

Table 2

Site characteristics, model parameters employed and calculated drought stress for the two validation stands. Values within square brackets and braces for *Prades* indicate model parameters and drought stress values obtained after setting soil depth to 80 cm and considering an additional rocky layer (85% of rocks), respectively.

	Vallcebre	Prades
Location (coordinates)	42°12'N, 1°49'E	41°19'N, 1#4–9#E
Altitude (m a.s.l.)	1260	1015
Mean annual temperature (°C)	7.3	11.3
Mean annual rainfall (mm)	862	664
Vegetation parameters		
Species	<i>Pinus sylvestris/Buxus sempervirens</i>	<i>P. sylvestris/Quercus ilex</i> / R+S-
Height	11 m/2 m	14 m/6 m/2 m
LAI	2.4/0.3	0.54/2.69/0.2
Root volume in topsoil (%)	62/60	65/66/66 [74/74/69] {68/68/60}
k_{sp}	0.5/0.4	0.5/0.55/0.4
b_{sp} (%)	66/10	66/50/10
s_{sp} (mm · LAI ⁻¹)	1.0/0.25	1.0/0.5/0.25
Ψ_{sp} (MPa)	-2.0 / -4.0	-2.0 / -3.0 / -4.0
S_{GDD}	-/-	-/-
Soil parameters		
Soil depth (topsoil + subsoil)	65 cm (30 + 35 cm)	40 cm (30 + 10 cm) [80 cm (30 + 50 cm)] {80 cm + rocky layer down to 4.5 m}
Topsoil texture (% sand, silt, clay)	(59, 19, 22)	(47, 32, 21)
Topsoil bulk density (kg dm ⁻³)	1.23	0.98
Topsoil macroporosity (%)	27	33
Topsoil rock fragment content (%)	19	45
Subsoil texture (% sand, silt, clay)	(62, 20, 18)	(48, 33, 19)
Subsoil bulk density (kg dm ⁻³)	1.48	1.48
Subsoil macroporosity (%)	14	11
Subsoil rock fragment content (%)	19	51
Max. soil evaporation (mm day ⁻¹)	1	2
Water volume at field capacity (mm)	122	54 [102]{238}
Predicted drought stress		
Average drought intensity (DI)	0.06/0.00	0.40/0.35/0.27 [0.33/0.27/0.17] {0.26/0.21/0.11}
Average drought duration (NDD)	32/0	151/141/128 [154/141/116] {148/133/97}

corresponding to maximum transpiration under average climatic conditions (see details in Section 2.6).

A three-year period (2003–2005 and 2011–2013 in *Vallcebre* and *Prades*, respectively) was used for validation and meteorological input data (daily temperature, rainfall and radiation) were obtained from on-site meteorological stations (Latron et al., 2010). Detailed descriptions regarding soil moisture and transpiration measurements for the validation period can be found in Poyatos et al. (2007), Poyatos et al. (2013), García-Estríngana et al. (2013) and Sus et al. (2014). Predicted vs. observed values were compared using linear regression analyses.

2.4. Forest inventory data and LAI estimation

Surveys of the Second Spanish Forest Inventory (SFI2) were conducted in Catalonia between 1989 and 1991 (Villaescusa and Díaz, 1998), while those of the Third Spanish Forest Inventory (SFI3) were conducted between 2000 and 2001 (Villanueva 2004). SFI2 and SFI3 surveys include 11,282 and 11,454 forest plots, respectively. In this study we considered the 8977 plots that were sampled in both SFI2 and SFI3 (Fig. 1), except for the determination of soil depth effects where we used all SFI3 plots located in areas where soil depth was available (see Section 2.8).

In both surveys, forest plots had been divided into four nested circular subplots (radius 5, 10, 15 and 25 m); and trees had been recorded only if their diameter was larger than a threshold (7.5, 12.5, 22.5 and 42.5, respectively). Species identity, height and diam-

eter at breast height (d.b.h.) of living and standing dead trees were available for both surveys. In the circular plot of 5 m radius, the number of saplings per species (2.5 cm ≤ d.b.h. < 7.5 cm) and their mean height had also been recorded. Species identity, canopy cover and mean height of woody understory vegetation had been sampled within the 10 m radius plot.

We assumed that each tree or shrub record was representative of a distinct plant cohort. Species identity and plant height, two parameters required in the model, were directly available from plot records. In order to obtain LAI estimates for trees, we calculated the basal area of each tree cohort and multiplied it by the slope of a species-specific linear regression with zero intercept against basal area (Table 1; see also Fig. S3.1 in Appendix S3), calibrated using data from Burriel et al. (2004). For shrubs, cover values were simply multiplied by 0.02 (i.e., 100% cover equals to LAI = 2). Estimation of root distribution is explained in Section 2.6.

2.5. Climatic and soil data

Temperature (in °C), rainfall (in mm) and mean daily solar radiation (in 10 kJ m⁻² day⁻¹) data, spatially interpolated at 1 km resolution (Ninyerola et al., 2000), were obtained for each month in the 1980–2010 period from the Spanish Meteorological Agency (AEMET) and the Catalan Meteorological Service (SMC). Daily temperature and daily solar radiation were simply interpolated linearly between average monthly values, whereas daily rainfall values were generated by sequentially drawing values from a Gamma

distribution (shape = 2, scale = 4) until the monthly precipitation demand was met (model sensitivity to parameters of this distribution is included in Appendix S2). The ratio between the evaporation rate and the rainfall rate (a parameter needed for rainfall interception loss; see Appendix S1) was set to 0.2 between December and June and to 0.05 between July and November (Miralles et al., 2010).

Soil was poorly characterized in SFI2; and field surveys of SFI3 only included qualitative descriptions of soil texture, litter content and surface rock abundance. The percentage of rocks in the surface of the plot was taken as a proxy of rock fragment content in the soil. Soil texture and bulk density corresponding to the topsoil and subsoil (0–30 cm and 30–100 cm) were obtained from spatial layers from the Harmonized World Soil Database (FAO/IIASA/ISRIC/ISS-CAS/JRC, 2009). Bulk density and the percent of sand were used to calculate macroporosity (Stolf et al., 2011). While being a key parameter for water balance, soil depth varies strongly at fine scale and is difficult to estimate accurately. To avoid overestimation of drought stress, we took a conservative approach and set soil depth (topsoil + subsoil) to 100 cm for all forest inventory plots (but we compared stress estimates in areas with available soil depth data, see Section 2.8).

2.6. Root distribution

Plant roots can be quite deep in semi-arid and Mediterranean ecosystems (Canadell et al., 1996; Schenk and Jackson, 2002). Although root architecture is species-specific, abiotic and biotic factors have a profound influence on root growth and structure (Casper and Jackson, 1997). Unfortunately, plant root systems are rarely sampled in forest inventories. We estimated root distribution among soil layers by finding the distribution that maximized plant transpiration in the model (preliminary analyses in which drought stress was minimized gave similar results) (Collins and Bras, 2007; Kleidon and Heimann, 1998). In the linear dose response model the distribution of roots is governed by parameters D50 and D95, the depths above which 50% and 95% of root mass is located, respectively (Schenk and Jackson, 2002). We explored the same state-space used in Collins and Bras (2007) and determined the D50/D95 pair corresponding to a maximum transpiration over three years of model simulation.

We determined optimum root distribution for each forest plot and each species separately. In each case, we used a single plant cohort of the target species with a LAI value equal to the LAI of the whole stand (thus, we assumed optimum root systems to be independent of the identity of neighbors). The factors that influenced the optimum root distribution of a given species in a given plot were: (i) species-specific model parameters (Ψ_{sp} , but also s_{sp} because it influenced soil infiltration); (ii) the LAI of the target stand; (iii) climatic conditions, soil texture and rock fragment content in the target plot. Pseudo-daily meteorological data for the optimization process was generated using average monthly values obtained from the Catalan Digital Climatic Atlas (Ninyerola et al., 2000; Pons and Ninyerola, 2008).

2.7. Model runs

All simulations started with soil layers at field capacity. Although all plant cohorts compete for water resources in the model, we evaluated drought stress for tree species only. Since the model produces DI and NDD values at the plant cohort level, drought stress values corresponding to each species and plot were obtained by averaging the stress values of plant cohorts of the plot corresponding to the same species, using LAI values as weights. We accounted for uncertainty derived from the stochastic generation of daily precipitation by averaging DI and NDD values across ten model runs. Preliminary analyses indicated that ten replicates cor-

respond to a standard error of around 0.001 for the DI average and less than one day for the NDD average.

2.8. Bias in drought stress estimates derived from assuming constant soil depth

In our application of the model to Catalonia we assumed a constant soil depth of 100 cm for all forest plots. To quantify the bias in drought stress derived from a lack of soil depth data in the study area, we used 1435 SFI3 plots located within three catchments where soil depth estimates were available, including 347 SFI3 plots that had not been surveyed in SFI2 (Fig. 1). Soil depth spatial layers in these catchments had been obtained from local soil maps complemented with estimates of regression models between soil profile data and soil units (CREAF/UPC/ETC/IRTA, 2011). Drought stress predictions for the year of SFI3 survey (either 2000 or 2001) were calculated assuming 100 cm soil depth and using actual soil depth estimates. Species optimum root distributions were determined separately for both soil depths.

2.9. Bias in drought stress estimates derived from temporal extrapolation

Our approach to assess drought stress relies on static information about forest structure and composition. Hence, drought stress estimates can have a substantial bias when conducted several years after the year of forest survey. To measure the bias derived from assuming constant structure and composition in forest plots, we took the 8977 re-measured plots and calculated DI and NDD predictions using SFI2 data for the year of the SFI3 survey and compared them with those obtained using SFI3 data. As before, species optimum root distributions were estimated separately for SFI2 and SFI3, with the aim to emulate the plasticity of root systems to adapt to changes in aboveground structure. An increase in drought stress between forest inventories was expected as a result of tree growth and forest densification; whereas decreases in drought stress were expected in stands subjected to decreases in basal area, for example after management or natural disturbances. We calculated Spearman's rank correlation to test the relationship between the difference in predicted drought stress and the corresponding SFI3-SFI2 difference in stand's LAI.

2.10. Temporal trends in climate and plant drought stress

We characterized 1980–2010 temporal trends in mean annual temperature, annual precipitation and climatic drought for all SFI3 plots. Climatic drought was calculated using the Standardized Precipitation-Evapotranspiration Index (SPEI; Vicente-Serrano et al., 2010; Beguería and Vicente-Serrano, 2013), a multiscalar index whose calculation involves a monthly climatic water balance series. For SPEI calculations, monthly PET was obtained adding the daily values used in the model and the scale of the index was 12 months.

Using the water balance model and the 8977 re-measured plots, we characterized trends in drought stress for each species by combining drought stress predictions obtained using SFI2 data (1989–1999 period) and SFI3 data (1991–2010 period). Drought stress during the 1991–1999 period was defined as the average of SFI2 and SFI3 predictions using weights that depended on the year (for example, SFI2 and SFI3 predictions had 0.9 and 0.1 weights, respectively, for year 1991; and the reverse weights were used for year 1999). With the aim to distinguish drought stress changes driven by climate from changes derived from changes in LAI, we compared the trends predicted as explained above with those obtained using SFI2 data for the whole period (1980–2010). In all cases the Mann–Kendall trend test (Mann, 1945) was used to deter-

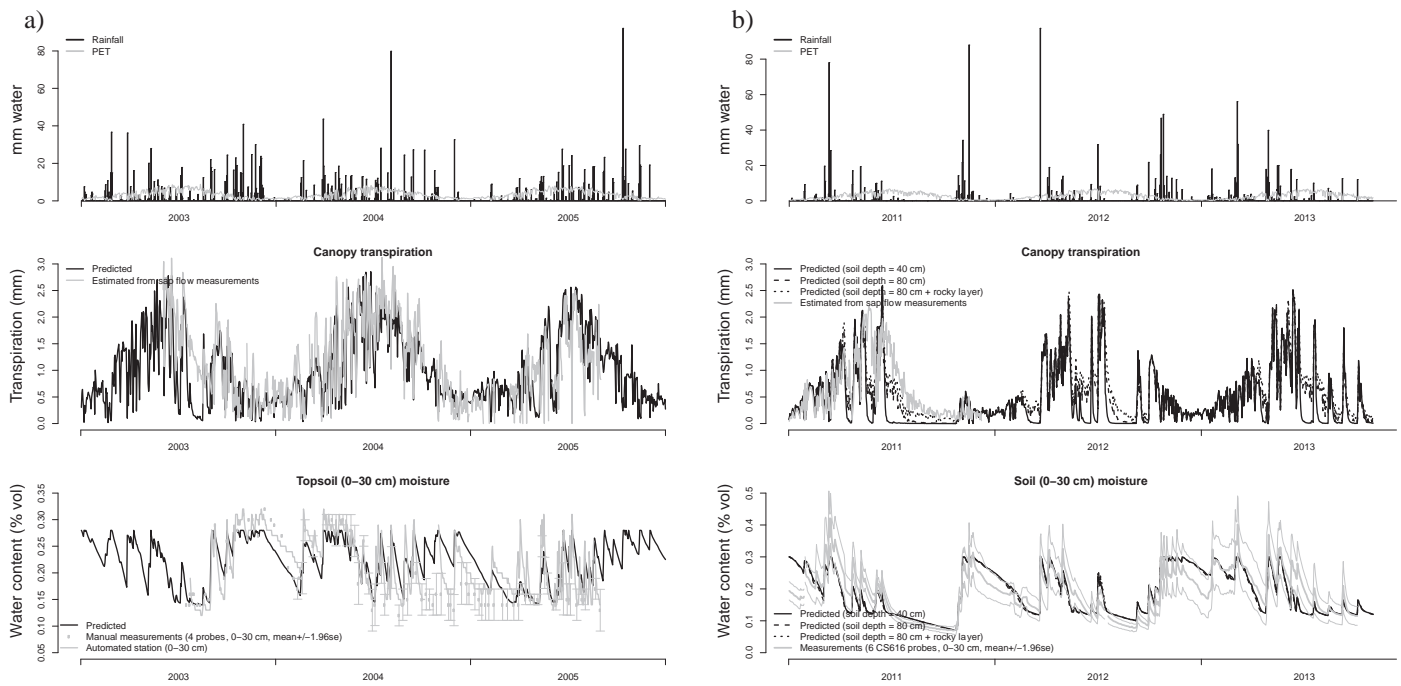


Fig. 2. Meteorological input (top), canopy transpiration (center) and topsoil moisture (bottom) at *Vallcebre* (a) and *Prades* (b) stands. Center and bottom panels include the comparison between observed values (in gray) and model predictions (in black).

mine the statistical significance of trends (significance level was set to $P=0.05$) and the magnitude of the trend was assessed using the Theil–Sen approach (Sen, 1968).

3. Results

3.1. Model evaluation

Predicted daily canopy transpiration values in *Vallcebre* site matched reasonably well the transpiration estimation obtained from sap flow measurements ($a=0.289$; $b=0.831$; $r^2=0.61$), except during the summer 2003 drought (Fig. 2a). Predicted topsoil moisture variations also matched moderately well with both manual ($a=0.010$; $b=0.836$; $r^2=0.41$) and automatic ($a=0.006$; $b=0.951$; $r^2=0.57$) field measurements (Fig. 2a). Topsoil moisture predictions for *Prades* site were rather strongly correlated with field mea-

surements ($a=0.030$; $b=0.835$; $r^2=0.69$). Canopy transpiration was clearly underestimated during drought periods when using 40 cm soil depth ($a=0.429$; $b=0.527$; $r^2=0.25$) (Fig. 2b). However, the fit to observed transpiration improved when increasing soil depth to 80 cm ($a=0.265$; $b=0.789$; $r^2=0.51$) or when considering an additional rocky layer (85% of rocks) extending down to 4.5 m ($a=0.171$; $b=0.886$; $r^2=0.62$). As expected, predicted drought stress was much higher in *Prades* than in *Vallcebre* (e.g., NDD = 151 vs. 32 days for *Pinus sylvestris*; Table 2).

3.2. LAI and root distribution estimates

Stand LAI values were significantly smaller under SFI2 (mean = 1.8; s.d. = 1.4) than under SFI3 (mean = 2.0; s.d. = 1.4) [p -value < 0.0001 in a Wilcoxon test]; and differences in LAI were highly variable among stands (s.d. = 0.95) (Fig. 3).

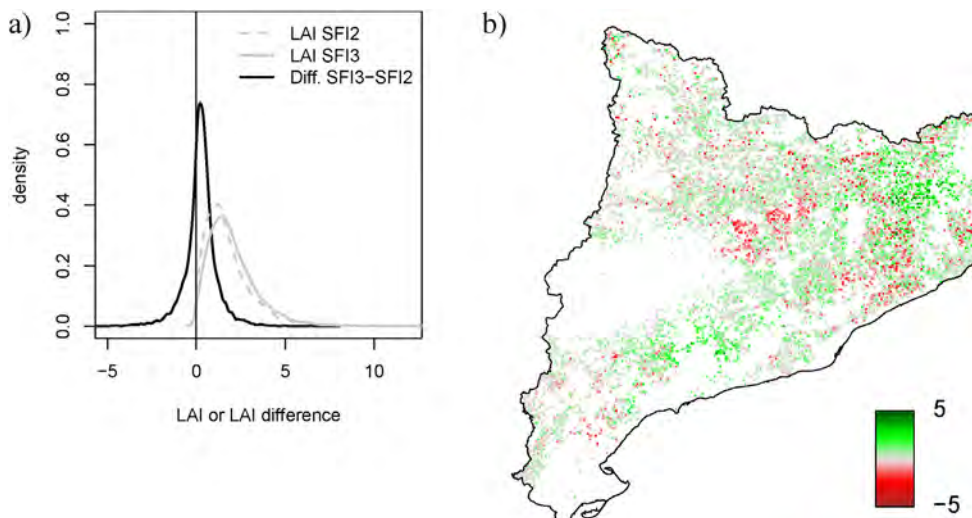


Fig. 3. (a) Density distribution of stand LAI values under SFI2 and SFI3, and distribution of LAI differences; (b) Spatial distribution of LAI changes.

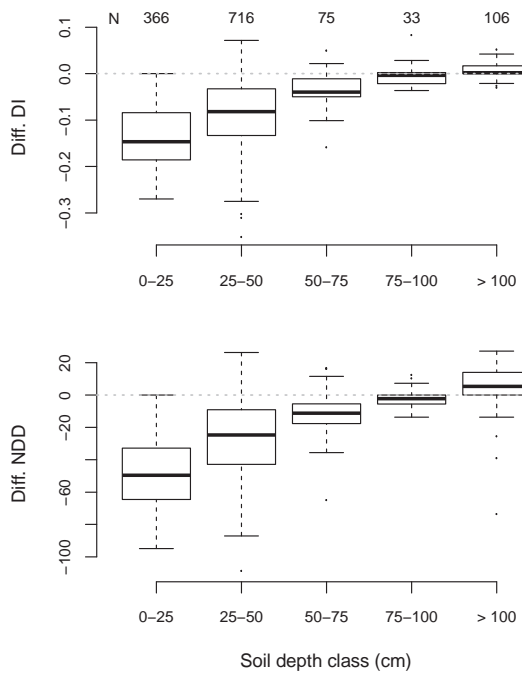


Fig. 4. Difference between drought stress values (DI and NDD) obtained assuming 100 cm soil depth for all plot records and drought stress values obtained using soil depth estimates available for three catchments (Fig. 1). N – Number of forest plots in each soil depth class.

In plots with fine-textured soils root biomass tended to concentrate in the topsoil, whereas in medium- or coarse-textured soils roots were mostly in the subsoil (see Fig. S4.1 in Appendix S4). Under arid conditions differences in root distribution due to soil texture were relatively small. In contrast, when climatic wetness increased root distribution became shallower in fine-textured soils and deeper for other textures. The density of the stand also had a strong effect on root distribution.

3.3. Bias in drought stress estimates derived from assuming 100 cm soil depth

Soil depths were generally lower than 100 cm in the three catchments where estimates were available. Therefore, the model tended to underestimate water stress for those stands (Fig. 4). Although we found high variation among plots, on average drought stress bias was rather small for soils deeper than 50 cm (i.e., less than 0.05 in DI and less than 15 days in NDD) and it rapidly increased for shallower soils. A very small overestimation of drought stress occurred for soils deeper than 100 cm.

3.4. Bias in drought stress estimates derived from temporal extrapolation

For most species, the regional average SFI2-SFI3 difference in predicted drought stress was negative (Fig. 5), indicating an underestimation of stress for assessments conducted with SFI2 data. Specifically, regional average differences in NDD ranged between −2 days and −17 days (corresponding to *Pinus uncinata* and *Quercus pubescens*, respectively) differences in DI ranged between −0.001 and −0.023 (corresponding to *P. uncinata* and *Pinus halepensis*, respectively).

Drought stress differences varied strongly among forest plots; and correlations with changes in stand LAI were substantial (Spearman's ρ between −0.39 and −0.73 for DI and between −0.22

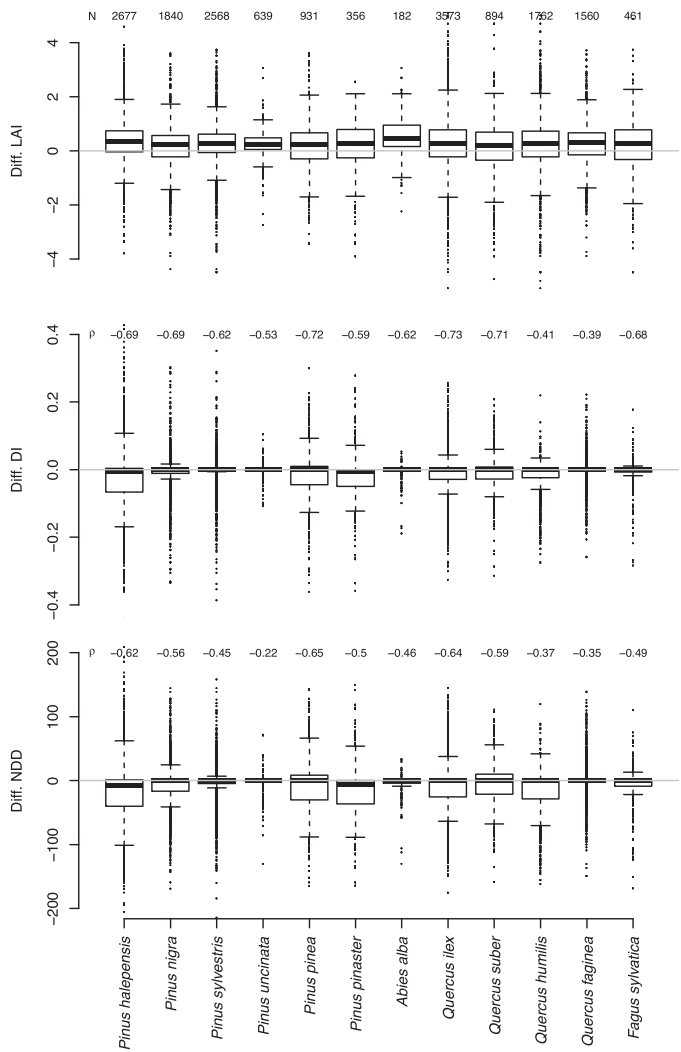


Fig. 5. Differences between SFI2 and SFI3 in stand LAI (top), DI (center) and NDD (bottom). For each species, a boxplot shows the values of all plot records where the species is present. N – Number of forest plots where the species occurs; ρ – Spearman's correlation coefficient between differences in drought stress and differences in stand LAI.

and −0.65 for NDD, depending on the species; Fig. 5). Among-plot variation in stand LAI differences was rather similar among species. In contrast, among-plot variation in drought stress changes between forest inventories was larger for Mediterranean species (*P. halepensis*, *Pinus pinea*, *Pinus pinaster*, *Quercus ilex* and *Quercus suber*) and progressively smaller for species corresponding to sub-Mediterranean (*Pinus nigra*, *Quercus humilis* and *Quercus faginea*), temperate (*P. sylvestris*, *Fagus sylvatica*, *Abies alba*) and mountainous (*P. uncinata*) climates.

3.5. Temporal trends in climatic drought and tree drought stress in Catalonia

During the period 1980–2010, 42% of forest plots in the study area experienced significant increase in mean annual temperature; and only 0.2% experienced a decrease (mean change = +0.63 °C; s.d. = 0.40 °C) (Fig. 6a). In contrast, we found that only a few plots had experienced changes in annual precipitation (0.6% and 0.2% of plots with significant increase and decrease, respectively) and average precipitation changes in the region were relatively small (mean change = +11 mm, s.d. = 64 mm) (Fig. 6b). Regarding SPEI (scale = 12

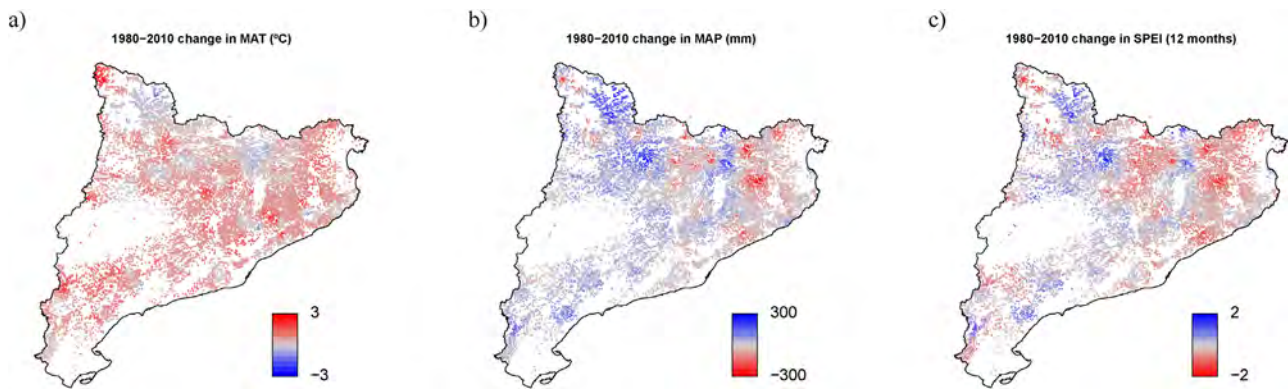


Fig. 6. Changes in mean annual temperature (MAT, in °C), mean annual precipitation (MAP, in mm) and the Standardized Precipitation-Evapotranspiration Index (SPEI, scale = 12 months) for the period 1980–2010. Trend analyses were conducted following the Theil-Sen approach.

months) we found a small tendency towards aridification (mean change = -0.13 , s.d. = 0.45), with a significant aridification trend for 28.1% of plots and a significant decrease of aridity for 10.6% of plots (Fig. 6c).

The water balance model predicted an increase in drought stress during the period 1980–2010 for most tree species (Figs. 7 and 8), in accordance with the results obtained in Subsection 3.4. For example, NDD increased for *P. halepensis* in 34% of the plots where the species was present while it decreased in 9% of plots. On average, annual drought duration increased in 17 days for this species, although with a very large variability among plots (s.d. = 64 days). At the other extreme, NDD increased for *P. uncinata* for 4% of plots only, while it decreased for 0.5% of plots; and the average change in drought duration was a decrease of 1 day (s.d. = 10 days). Appendix S4 shows among-plot variation and the spatial distribution of both

average drought stress and the magnitude of stress changes for the period studied.

When we determined trends in drought stress using SFI2 data alone (hence, assuming no change in forest structure during the studied period), we found very few changes in drought stress (between 0% and 1.7% of plots with an increase in NDD, and between 0% and 2.3% with an increase in DI, depending on the species) (Figs. 7 and 8). Moreover, changes in drought stress correlated moderately well with climatic changes when using SFI2 data alone; but they almost did not when both forest inventories were used. For example, Pearson's correlation between the 1980–2010 changes in SPEI and the corresponding changes in DI was $r = -0.40$ for *Q. ilex* when trends in DI were obtained assuming constant forest structure. In contrast, the same correlation was $r = -0.13$ when the change in forest structure was taken into account.

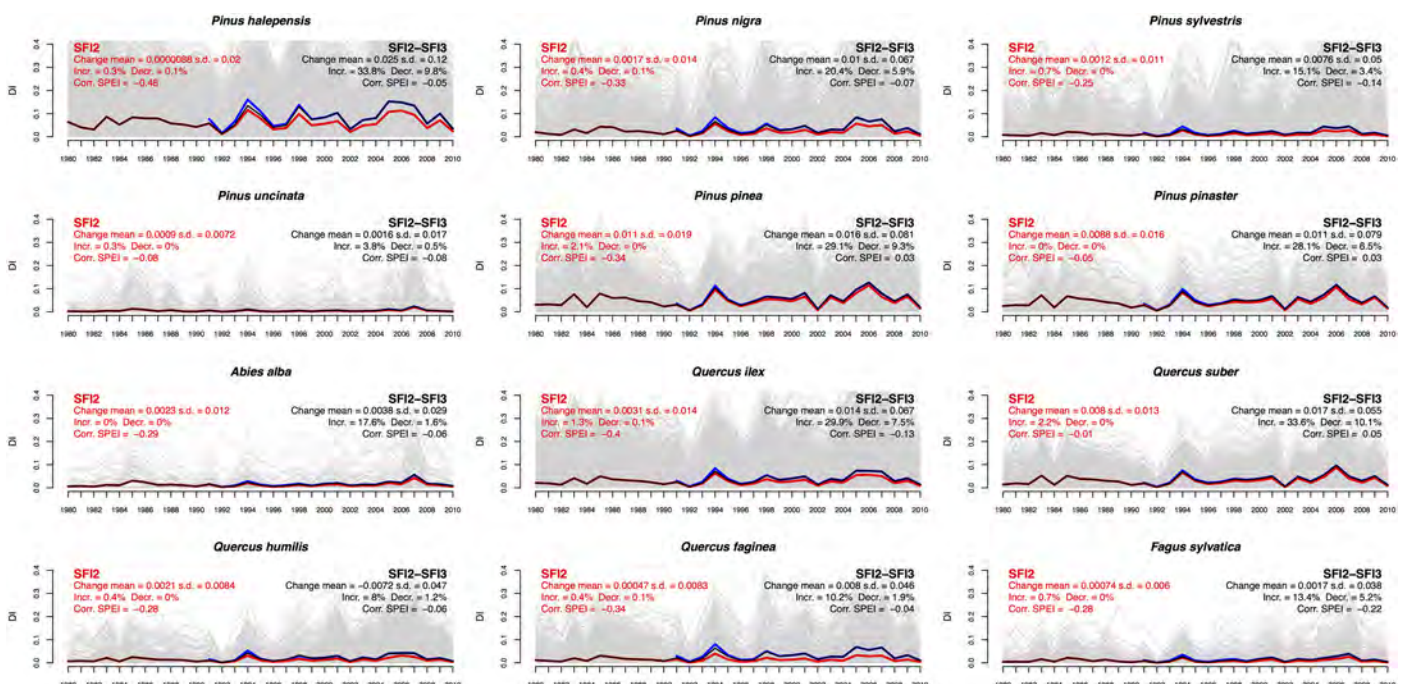


Fig. 7. Temporal trends in drought intensity (DI) for all studied species during the period 1980–2010. Red and blue lines indicate average trends calculated using SF12 data or SF13 data, respectively. Black lines indicate average trends obtained after combining predictions for both forest inventories. Trends for individual forest plots are shown in light grey. Change mean and s.d. – Mean and standard deviation of the magnitude of change in DI, according to the Theil-Sen approach. Incr./Decr. – Percentage of plots (among those where the species is present) with significant increase/decrease ($P < 0.05$) in DI, according to the Mann-Kendall trend test. Corr. SPEI – Pearson correlation between the slope of DI and the slope of Standardized Precipitation-Evapotranspiration Index (scale = 12 months). (For interpretation of the references to colour in this figure legend, the reader is referred to the web version of this article.)

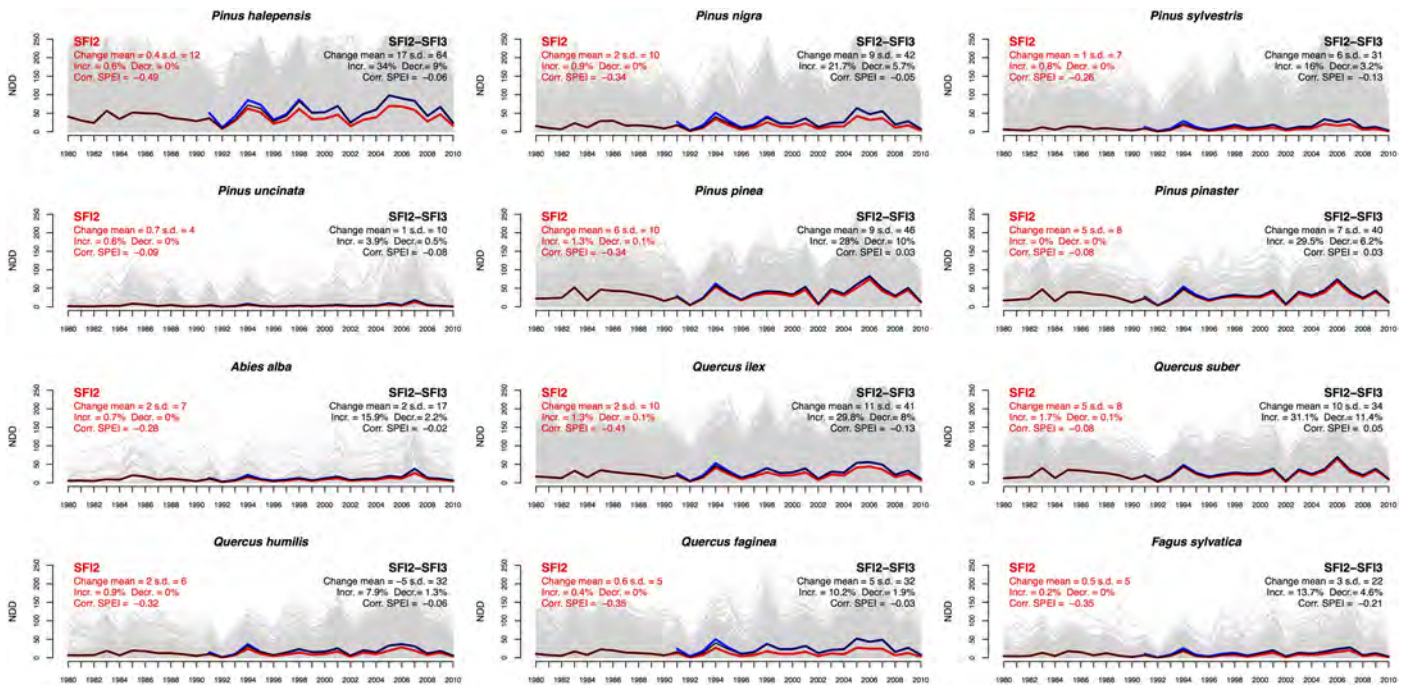


Fig. 8. Temporal trends in number of drought days (NDD) for all studied species during the period 1980–2010. Red and blue lines indicate average trends calculated using SF12 data or SF13 data, respectively. Black lines indicate average trends obtained after combining predictions for both forest inventories. Trends for individual forest plots are shown in light grey. Change mean and s.d. – Mean and standard deviation of the magnitude of change in NDD, according to the Theil–Sen approach. Incr./Decr. – Percentage of plots (among those where the species is present) with significant increase/decrease ($P < 0.05$) in NDD, according to the Mann–Kendall trend test. Corr. SPEI – Pearson correlation between the slope of NDD and the slope of the Standardized Precipitation–Evapotranspiration Index (scale = 12 months). (For interpretation of the references to colour in this figure legend, the reader is referred to the web version of this article.)

4. Discussion

4.1. Recent trends of drought stress in Catalonia

Our model predicted an increase in intensity and duration of drought stress for most tree species in Catalonia, but we found that changes in drought stress mostly originated from changes in leaf area rather than from climatic aridification. Since the mid twentieth century, forest cover in the northwest Mediterranean Basin is increasing due to the progressive colonization of former agricultural areas and the densification of pre-existing forests associated to the decrease of forest management activities (Améztegui et al., 2010; Weissteiner et al., 2011). One of the consequences of this fuel accumulation is the increased frequency of large wildfires (Pausas, 2004; Pausas and Fernández-Muñoz, 2012); the largest ones in Catalonia occurred between the two SFI inventories (Díaz-Delgado et al., 2004). The footprint of those events is clear in the spatial distribution of LAI changes, but does not compensate for the increase in LAI over most of the region (Fig. 3). Mortality rates in the Iberian Peninsula have been associated to forest densification in dry sites (Vilà-Cabrera et al., 2011; Vayreda et al., 2012; Ruiz-Benito et al., 2013). Our results support the idea that increasing forest management could reverse the observed general increase in drought stress, regardless of the observed increase in temperatures (Cotillas et al., 2009). This would, in turn, lower fire risk as fires in the study area are partially controlled by fuel (Pausas & Fernández-Muñoz, 2012; Pausas and Paula, 2012).

On average, Mediterranean tree species were predicted to experience higher intensity and duration of drought stress than sub-Mediterranean or temperate species. These results do not imply that Mediterranean plants are more likely to exhibit drought stress effects, because their ability to tolerate stress is much higher. Choat et al. (2012) recently showed that many tree species oper-

ate with narrow hydraulic safety margins against injurious levels of drought stress and that these safety margins are unrelated to rainfall regimes at global scale. This view is also supported by recent observations of crown defoliation not being restricted to the most drought-sensitive species but affecting all tree species examined (Carnicer et al., 2011). If we neglect intraspecific variation in drought resistance, one should expect larger drought-related effects for a given species in those stands where climatic, soil and vegetation conditions lead to unusually high stress values with respect to those found across the distribution of the species (see Figs. S4.4 and S4.6 in Appendix S4). For example, the 151 days of drought stress for *P. sylvestris* in the Prades validation stand, where high mortality rates have been observed since the 1990s (Martínez-Vilalta and Piñol, 2002; Poyatos et al., 2013), corresponds to 99.7% in the cumulative distribution of NDD for this species in Catalonia.

4.2. Potential applications

We have shown that running a process-based model on forest inventory plots can be used to obtain species-specific estimates of drought stress at landscape and regional scales. This approach could be adopted to identify areas where the combination of forest structure, species composition, soil conditions and current climate makes them highly vulnerable to drought impacts. In addition, when coupled with daily meteorological data (and assuming repeated forest inventory surveys), this approach could be used to routinely monitor plant drought stress over large areas, complementing remote sensing indices that are normally used to monitor the effects of drought stress (Deshayes et al., 2006). Using daily meteorological data would avoid the need to conduct temporal downscaling, which in our case involved many assumptions such as the lack of correlation between temperature and precipitation. Compared to hydrological models that already provide soil moisture estimates in agricultural drought monitoring

(e.g., Sepulcre-Canto et al., 2012; Sheffield and Wood, 2008), our approach would provide species-specific drought stress estimates for forest systems. Finally, combining remote sensing technologies, such as LiDAR or multispectral imaging, with field data could be used to obtain spatially continuous information about forest structure (Holopainen and Kalliovirta, 2006; Estornell et al., 2011) and, hence, to generate drought stress predictions for stands not included in forest inventory plots.

Before promoting it for practical use to monitor drought stress at the regional scale, however, our model should be further validated by comparison of observed soil moisture and water fluxes in a larger number of stands spread over the region. Other regional-level validation exercises (e.g., the comparison between predicted stress and observed drought impacts or the comparison of modeled exported water with stream flow data) may be necessary but difficult to conduct due to the influence of additional processes (e.g., drought-related mortality or lateral water transfer) not currently implemented in the model.

4.3. Accuracy and temporal variation of LAI estimates

Modeling transpiration rates accurately is crucial for predicting soil moisture and drought stress variations; and transpiration rates primarily depend on LAI. In similar studies addressing drought stress patterns at the regional scale, Ruffault et al. (2013) relied on model-optimized LAI estimates, while Chakroun et al. (2014) used the relationship between field LAI values and remote sensing vegetation indices. In contrast with these studies, we estimated species-specific LAI values from forest inventory data using relationships between LAI and basal area (Table S2.1). While this approach can be more precise than using satellite-derived estimates, some biases may remain because the relationship between LAI and basal area is influenced by factors such as forest management (e.g., Davi et al., 2008; Le Dantec et al., 2000). Another limitation of using forest inventory data for LAI estimation is that LAI values are assumed to remain constant when computing drought stress before or after the year of survey. We found that the accuracy of our stand-level estimates was strongly dependent on this temporal extrapolation, although regional-level averages were much less sensitive (Fig. 5). Even if we exclude LAI changes derived from major changes in vegetation structure (e.g., forest encroachment, fire or human-mediated disturbances), plants are known to adjust their leaf area to cope with variations in drought stress (e.g., Le Dantec et al., 2000; Limousin et al., 2009; Maseda and Fernández, 2006). Accounting for drought-related LAI changes would require coupling water balance with carbon balance in the same model (e.g., Hoff and Rambal, 2003). Alternatively, combining forest inventory with remotely sensed data would allow tracking LAI variations caused by this or other processes (e.g., Chakroun et al., 2014).

4.4. Availability of belowground data

Availability of good quality belowground data is also important to increase the usefulness of our approach, because of the strong dependency of the water balance on rooting depth and soil characteristics like depth, texture or stoniness. Our results indicate that substantial biases in drought stress may occur when the depth of shallow soils (<50 cm) is overestimated. Ideally, soil attributes of forest plots should be obtained from forest inventory or other field surveys. Alternatively, spatial variation in soil attributes may be modeled from topographic, lithological and land use information (Boer et al., 1996; Zheng et al., 1996; Tesfa et al., 2009). Regarding root systems, solving for an optimized root distribution on the basis of environmental conditions produces estimates that may not be realistic, depending on the model definition. For example, our

model did not include any penalization derived from the energetic costs of creating and maintaining roots (Schymanski et al., 2008). Moreover, slightly different root distributions would have been obtained if we had chosen to minimize drought stress or maximize net primary production, instead of maximizing transpiration (Collins and Bras, 2007; Kleidon and Heimann, 1998). Given the difficulty to obtain root profiles in the field for even a moderate number of forest stands, we think that the strategy of optimizing root distributions provides an operational solution. An additional modeling issue arises because deep roots frequently occurs within rock fissures and cracks in sclerophyllous vegetation (Canadell et al., 1996; Keeley et al., 2012). Accounting for such additional soil water capacity may be important when modeling transpiration and drought stress in areas with shallow soils (Rambal et al., 2003; Ruffault et al., 2013), as we did the Prades site (in agreement with Barbeta et al., 2014).

4.5. Limitations of the current model design

In this study we opted for a process-based model where – compared to ecosystem models, land surface models or dynamic global vegetation models – many processes were highly condensed and others were simply absent. While this strategy facilitated calibration over the study area and provided satisfactory validation results, additional processes may need to be considered. We mentioned above that considering carbon balance would allow addressing temporal changes in LAI. Predictions of drought stress would likely be more accurate if the model included the down-regulation of stomata conductance derived from increased CO₂ concentrations (e.g., Dufrêne et al., 2005; Keenan et al., 2011). Distinguishing between plant cohorts in our model required splitting the maximum stand transpiration, calculated following Granier et al. (1999), among them. Experimental data would be necessary to calibrate species-specific relationships between LAI and maximum transpiration. The use of a radiation transfer module including other wavelengths than visible could provide a better estimation of the evapotranspiration fraction assigned to the understory (Balandier et al., 2006). Furthermore, whole-plant conductance was assumed to be independent of previous drought events (i.e., hysteresis was lacking in the relationship between soil water potential and plant conductance) (Limousin et al., 2009; Sus et al., 2014). Although seldom considered, hydraulic redistribution may buffer the effects of changes in soil moisture regimes and thereby increase the resilience of ecosystems to changes in patterns of precipitation (Horton and Hart, 1998; Weltzin et al., 2003). Finally, a one-dimensional (vertical) model like ours may inaccurately predict soil moisture dynamics when non-local controls (i.e., lateral transport by subsurface or overland flow) dominate (Grayson and Western, 1997). Incorporating lateral water transfer could have potentially lowered the amount of drought stress for some plots. However, in Mediterranean areas evapotranspiration exceeds precipitation during long periods and vertical fluxes dominate under these conditions (Garcia-Estrada et al., 2013; Grayson and Western, 1997).

4.6. From drought stress to drought impacts

Predicting drought-related events of tree decline or mortality resulting from expected climatic changes requires to effectively link drought stress estimates to drought-related effects. Predicting drought impacts is hampered by our incomplete knowledge on how drought stress changes demographic rates. For example, different species and life stages may respond to drought stress measured at different temporal scales (Pasho et al., 2011). Furthermore, drought-induced mortality can be in fact the result of drought stress interacting with other factors like pests and pathogens (McDowell

et al., 2011; Oliva et al., 2014), which may explain why attempts to predict the occurrence of mortality have been generally unsuccessful (McDowell et al., 2013). Physiological models can relate climatic variability with drought-related mortality at the individual and stand levels (e.g., Martínez-Vilalta et al., 2002; Zavala and Bravo de la Parra, 2005; Tague et al., 2013), but their predictive capacity remains to be tested at larger scales. Dynamic global vegetation models, gap models or landscape dynamics models may be useful to study drought impacts on vegetation structure and composition over large areas (e.g., Bugmann and Cramer 1998; Fyllas and Troumbis, 2009; Gustafson and Sturtevant, 2013; Mouillot et al., 2001), but further modeling efforts are needed to strengthen the link between predicted drought stress and actual demographic rates before they can be used to accurately predict drought impacts (Keane et al., 2001).

Acknowledgements

This study has received financial support from the projects CGL2011-29539, CGL2010-16373, CGL2012-39938-C02-01, CGL2013-46808-R and MONTES-Consolider CSD2008-00040 granted by the Spanish Ministry of Education and Science (MEC). This is a contribution to the ERA-NET INFORMED project. Additional support to M.D.C came from research contract granted by the Spanish Ministry of Economy and Competitiveness (RYC-2012-11109). We thank Miquel Ninyerola and Meritxell Batalla (Botany Department, Autonomous University of Barcelona) for generating spatially explicit climatic predictions from data provided by the Spanish Meteorological Agency and the Spanish Ministry of Marine and Rural Environment; and Jaume Fons (Geography Department, Autonomous University of Barcelona) for generating soil depth estimates. We also thank Assu Gil and Mario Beltrán (CTFC) for useful discussions and technical assistance.

Appendix A. Supplementary data

Supplementary data associated with this article can be found, in the online version, at <http://dx.doi.org/10.1016/j.agrformet.2015.06.012>

References

- Allen, C.D., Macalady, A.K., Chenchouni, H., Bachelet, D., McDowell, N., Vennetier, M., Kitzberger, T., Rigling, A., Breshears, D.D., Hogg (Ted), E.H., Gonzalez, P., Fensham, R., Zhang, Z., Castro, J., Demidova, N., Lim, J.-H., Allard, G., Running, S.W., Semerci, A., Cobb, N., 2010. A global overview of drought and heat-induced tree mortality reveals emerging climate change risks for forests. *For. Ecol. Manage.* 259, 660–684, <http://dx.doi.org/10.1016/j.foreco.2009.09.001>
- Améztegui, A., Brotons, L., Coll, L., 2010. Land-use changes as major drivers of mountain pine (*Pinus uncinata* Ram.) expansion in the Pyrenees. *Glob. Ecol. Biogeogr.* 19, 632–641, <http://dx.doi.org/10.1111/j.1466-8238.2010.00550.x>
- Aubin, I., Beaudet, M., Messier, C., 2000. Light extinction coefficients specific to the understory vegetation of the southern boreal forest, Quebec. *Can. J. For. Res.* 30, 168–177, <http://dx.doi.org/10.1139/x99-185>
- Balandier, P., Sonohat, G., Sinoquet, H., Varlet-Grancher, C., Dumas, Y., 2006. Characterisation, prediction and relationships between different wavebands of solar radiation transmitted in the understory of even-aged oak (*Quercus petraea* Q. robur) stands. *Trees* 20, 363–370.
- Barbeta, A., Mejía-Chang, M., Ogaya, R., Voltas, J., Dawson, T.E., Peñuelas, J., 2014. The combined effects of a long-term experimental drought and an extreme drought on the use of plant-water sources in a Mediterranean forest. *Global Change Biol.*, <http://dx.doi.org/10.1111/gcb.12785>
- Bartlett, M.K., Scoffoni, C., Sack, L., 2012. The determinants of leaf turgor loss point and prediction of drought tolerance of species and biomes: a global meta-analysis. *Ecol. Lett.* 15, 393–405, <http://dx.doi.org/10.1111/j.1461-0248.2012.01751.x>
- Beguería, S., Vicente-Serrano, S.M., 2013. SPEI: Calculation of the Standardised Precipitation-Evapotranspiration Index. R package version 1.6. <http://CRAN.R-project.org/package=SPEI>
- Boer, M., Barrio, G., Del Puigdefábregas, J., 1996. Mapping soil depth classes in dry Mediterranean areas using terrain attributes derived from a digital elevation model. *Geoderma* 72, 99–118.
- Boughton, W., 1989. A review of the USDA SCS curve number method. *Aust. J. Soil Res.* 27, 511–523.
- Bréda, N.J.J., 2003. Ground-based measurements of leaf area index: a review of methods, instruments and current controversies. *J. Exp. Bot.* 54, 2403–2417, <http://dx.doi.org/10.1093/jxb/erg263>
- Bugmann, H., Cramer, W., 1998. Improving the behaviour of forest gap models along drought gradients. *For. Ecol. Manage.* 103, 247–263.
- Burriel, J.A., Gracia, C., Ibáñez, J.J., Mata, T., Vayreda, J., 2004. *Inventari Ecològic Forestal de Catalunya*, 10 volumes. CREAF, Bellaterra, Spain.
- Canadell, J., Jackson, R., Ehleringer, J., Mooney, H., Sala, O., Schulze, E., 1996. Maximum rooting depth of vegetation types at the global scale. *Oecologia* 108, 583–595, <http://dx.doi.org/10.1007/BF00329030>
- Carnicer, J., Coll, M., Ninyerola, M., Pons, X., Sánchez, G., Peñuelas, J., 2011. Widespread crown condition decline, food web disruption, and amplified tree mortality with increased climate change-type drought. *Proc. Natl. Acad. Sci. U. S. A.* 108, 1474–1478, <http://dx.doi.org/10.1073/pnas.1010070108>
- Casper, B., Jackson, R., 1997. Plant competition underground. *Annu. Rev. Ecol. Syst.* 28, 545–570.
- Chakroun, H., Mouillot, F., Nasr, Z., Nouri, M., Ennajah, A., Ourcival, J.M., 2014. Performance of LAI-MODIS and the influence on drought simulation in a Mediterranean forest. *Ecohydrology* 7, 1014–1028.
- Choat, B., Jansen, S., Brodribb, T.J., Cochard, H., Delzon, S., Bhaskar, R., Bucci, S.J., Feild, T.S., Gleason, S.M., Hacke, U.G., Jacobsen, A.L., Lens, F., Maherli, H., Martínez-Vilalta, J., Mayr, S., Mencuccini, M., Mitchell, P.J., Nardini, A., Pittermann, J., Pratt, R.B., Sperry, J.S., Westoby, M., Wright, I.J., Zanne, A.E., 2012. Global convergence in the vulnerability of forests to drought. *Nature* 491, 752–755, <http://dx.doi.org/10.1038/nature11688>
- Collins, D.B.G., Bras, R.L., 2007. Plant rooting strategies in water-limited ecosystems. *Water Resour. Res.* 43, W06407, <http://dx.doi.org/10.1029/2006WR005541>
- Cotillas, M., Sabaté, S., Gracia, C., Espelta, J.M., 2009. Growth response of mixed mediterranean oak coppices to rainfall reduction. Could selective thinning have any influence on it? *For. Ecol. Manage.* 258, 1677–1683, <http://dx.doi.org/10.1016/j.foreco.2009.07.033>
- CREAF/UPC/ETC/IRTA, 2011. Adaptacions al Canvi Climàtic en l'Ús de l'Aigua.
- Dai, A., 2011. Drought under global warming: a review. *Wiley Interdiscip. Rev. Clim. Change* 2, 45–65, <http://dx.doi.org/10.1002/wcc.81>
- Davi, H., Baret, F., Huc, R., Dufrêne, E., 2008. Effect of thinning on LAI variance in heterogeneous forests. *For. Ecol. Manage.* 256, 890–899, <http://dx.doi.org/10.1016/j.foreco.2008.05.047>
- Davi, H., Dufrêne, E., Granier, A., Le Dantec, V., Barbaroux, C., François, C., Bréda, N., 2005. Modelling carbon and water cycles in a beech forest Part II.: Validation of the main processes from organ to stand scale. *Ecol. Modell.* 185, 387–405, <http://dx.doi.org/10.1016/j.ecolmodel.2005.01.003>
- Delzon, S., Cochard, H., 2014. Recent advances in tree hydraulics highlight the ecological significance of the hydraulic safety margin. *New Phytol.* 203, 355–358, <http://dx.doi.org/10.1111/nph.12798>
- Deshayes, M., Guyon, D., Jeanjean, H., Stach, N., Jolly, A., Hagolle, O., 2006. The contribution of remote sensing to the assessment of drought effects in forest ecosystems. *Ann. For. Sci.* 63, 579–595.
- Díaz-Delgado, R., Lloret, F., Pons, X., 2004. Spatial patterns of fire occurrence in Catalonia, NE, Spain. *Landsc. Ecol.* 19, 731–745, <http://dx.doi.org/10.1007/s10980-005-0183-1>
- Dufrêne, E., Davi, H., François, C., Maire, G., Le, Dantec, V., Granier, A., 2005. Modelling carbon and water cycles in a beech forest Part I: model description and uncertainty analysis on modelled NEE. *Ecol. Modell.* 185, 407–436, <http://dx.doi.org/10.1016/j.ecolmodel.2005.01.004>
- Estornell, J., Ruiz, L., Velázquez-Martí, B., 2011. Study of shrub cover and height using LiDAR data in a Mediterranean area. *For. Sci.* 57, 171–179.
- FAO/IIASA/ISRIC/ISS-CAS/JRC, 2009. Harmonized World Soil Database (version 1.1). FAO, Rome, Italy and IIASA, Laxenburg, Austria.
- Fyllas, N.M., Troumbis, A.Y., 2009. Simulating vegetation shifts in north-eastern Mediterranean mountain forests under climatic change scenarios. *Glob. Ecol. Biogeogr.* 18, 64–77, <http://dx.doi.org/10.1111/j.1466-8238.2008.00419.x>
- Garcia-Estrada, P., Latron, J., Llorens, P., Gallart, F., 2013. Spatial and temporal dynamics of soil moisture in a Mediterranean mountain area (Vallecebre, NE Spain). *Ecohydrology* 753, 741–753, <http://dx.doi.org/10.1002/eco.1295>
- Gash, J., Lloyd, C., Lachaud, G., 1995. Estimating sparse forest rainfall interception with an analytical model. *J. Hydrol.* 170.
- Gao, B.C., 1996. NDWI - a normalized difference water index for remote sensing of vegetation liquid water from space. *Remote Sens. Environ.* 58, 257–266, [http://dx.doi.org/10.1016/S0034-4257\(96\)673](http://dx.doi.org/10.1016/S0034-4257(96)673)
- Gobron, N., Pinty, B., Taberner, M., Mélin, F., Verstraete, M.M., Widlowski, J.L., 2006. Monitoring the photosynthetic activity of vegetation from remote sensing data. *Adv. Sp. Res.* 38, 2196–2202, <http://dx.doi.org/10.1016/j.asr.2003.07.079>
- Granier, A., Bréda, N., Biron, P., Villette, S., 1999. A lumped water balance model to evaluate duration and intensity of drought constraints in forest stands. *Ecol. Modell.* 116, 269–283.
- Granier, A., Reichstein, M., Bréda, N., Janssens, I.A., Falge, E., Ciais, P., Grünwald, T., Aubinet, M., Berbigier, P., Bernhofer, C., Buchmann, N., Facini, O., Grassi, G., Heinesch, B., Ilvesniemi, H., Kerone, P., Knöhl, A., Köstner, B., Lagergren, F., Lindroth, A., Longdoz, B., Loustau, D., Mateus, J., Montagnani, L., Nys, C., Moors, E., Papale, D., Peiffer, M., Pilegaard, K., Pita, G., Pumpanen, J., Rambal, S., Rebmann, C., Rodrigues, A., Seufert, G., Tenhunen, J., Vesala, T., Wang, Q., 2007. Evidence for soil water control on carbon and water dynamics in European

- forests during the extremely dry year: 2003. *Agric. For. Meteorol.* 143, 123–145, <http://dx.doi.org/10.1016/j.agrformet.2006.12.004>
- Grayson, R., Western, A., 1997. Preferred states in spatial soil moisture patterns: Local and nonlocal controls. *Water Resour. Res.* 33, 2897–2908.
- Gustafson, E.J., Sturtevant, B.R., 2013. Modeling forest mortality caused by drought stress: Implications for climate change. *Ecosystems* 16, 60–74, <http://dx.doi.org/10.1007/s10021-012-9596-1>
- Heim, R.R., 2002. Century drought indices used in the United States. *Bull. Am. Meteorol. Soc.*, 1149–1165.
- Hoff, C., Rambal, S., 2003. An examination of the interaction between climate, soil and leaf area index in a *Quercus ilex* ecosystem. *Ann. For. Sci.* 60, 153–161, <http://dx.doi.org/10.1051/forest>
- Holopainen, M., Kalliovirta, J., 2006. *Modern data acquisition for forest inventories. In: Kangas, A., Maltamo, M. (Eds.), Forest Inventory - Methodology and Applications*. Springer, Netherlands, pp. 343–362.
- Horton, J., Hart, S., 1998. Hydraulic lift: a potentially important ecosystem process. *Trends Ecol. Evol.* 13, 232–235.
- Jarvis, P., McNaughton, K., 1986. Stomatal control of transpiration: scaling up from leaf to region. *Adv. Ecol. Res.* 15, 1–49.
- Joffre, R., Rambal, S., 1993. How tree cover influences the water balance of Mediterranean rangelands. *Ecology* 74, 570–582.
- Keane, R., Austin, M., Field, C., Huth, A., 2001. Tree mortality in gap models: application to climate change. *Clim. Change* 51, 509–540.
- Keeley, J.E., Bond, W.J., Bradstock, R.A., Pausas, J.G., Rundel, P.W., 2012. *Fire in Mediterranean Ecosystems*. Cambridge University Press, New York.
- Keenan, T., Maria Serra, J., Lloret, F., Ninyerola, M., Sabate, S., 2011. Predicting the future of forests in the Mediterranean under climate change, with niche- and process-based models: CO₂ matters! *Global Change Biol.* 17, 565–579, <http://dx.doi.org/10.1111/j.1365-2486.2010.02254.x>
- Kerr, Y.H., Waldteufel, P., Richaume, P., Wigneron, J.P., Ferrazzoli, P., Mahmoodi, A., Bitar, A., Al Cabot, F., Gruber, C., Juglea, S.E., Leroux, D., Mialon, A., Delwart, S., 2012. The SMOS soil moisture retrieval algorithm. *Geosci. Remote Sens.* 50, 1384–1403.
- Kleidon, A., Heimann, M., 1998. A method of determining rooting depth from a terrestrial biosphere model and its impacts on the global water and carbon cycle. *Global Change Biol.* 4, 275–286, <http://dx.doi.org/10.1046/j.1365-2486.1998.00152.x>
- Klein, T., 2014. The variability of stomatal sensitivity to leaf water potential across tree species indicates a continuum between isohydric and anisohydric behaviours. *Funct. Ecol.* 28, 1313–1320, <http://dx.doi.org/10.1111/1365-2435.12289>
- Kogan, F.N., 1997. Global drought watch from space. *Bull. Am. Meteorol. Soc.* 78, 621–636.
- Latron, J., Llorens, P., Soler, M., Poyatos, R., Rubio, C., Muzylo, A., Martínez-Carreras, N., Delgado, J., Regués, D., Catari, G., Nord, G., Gallart, F., 2010. Hydrology in a Mediterranean mountain environment-The Valcaba research basins (North Eastern Spain). I. 20 years of investigations of hydrological dynamics. *IAHS Publ.* 336, 38–43.
- Lafont, S., Zhao, Y., Calvet, J.C., Peylin, P., Ciais, P., Maignan, F., Weiss, M., 2012. Modelling LAI, surface water and carbon fluxes at high-resolution over France: comparison of ISBA-A-gs and ORCHIDEE. *Biogeosciences* 9, 439–456, <http://dx.doi.org/10.5194/bg-9-439-2012>
- Lindner, M., Maroschek, M., Netherer, S., Kremer, A., Barabti, A., Garcia-Gonzalo, J., Seidl, R., Delzon, S., Corona, P., Kolström, M., Lexer, M.J., Marchetti, M., 2010. Climate change impacts, adaptive capacity, and vulnerability of European forest ecosystems. *For. Ecol. Manage.* 259, 698–709, <http://dx.doi.org/10.1016/j.foreco.2009.09.023>
- Le Dantec, V., Dufrêne, E., Saugier, B., 2000. Interannual and spatial variation in maximum leaf area index of temperate deciduous stands. *For. Ecol. Manage.* 134, 71–81, [http://dx.doi.org/10.1016/S0378-1127\(99\)246-7](http://dx.doi.org/10.1016/S0378-1127(99)246-7)
- Le Maire, G., Davi, H., Soudani, K., François, C., Le Dantec, V., Dufrêne, E., 2005. Modeling annual production and carbon fluxes of a large managed temperate forest using forest inventories, satellite data and field measurements. *Tree Physiol.* 25, 859–872.
- Limousin, J.M., Rambal, S., Ourcival, J.M., Rocheteau, A., Joffre, R., Rodriguez-Cortina, R., 2009. Long-term transpiration change with rainfall decline in a Mediterranean *Quercus ilex* forest. *Global Change Biol.* 15, 2163–2175, <http://dx.doi.org/10.1111/j.1365-2486.2009.01852.x>
- Lischke, H., Zimmermann, N.E., Bolliger, J., Rickebusch, S., Löfller, T.J., 2006. TreeMig: a forest-landscape model for simulating spatio-temporal patterns from stand to landscape scale. *Ecol. Model.* 199, 409–420, <http://dx.doi.org/10.1016/j.ecolmodel.2005.11.046>
- Mann, H., 1945. Nonparametric tests against trend. *Econometrica* 13, 245–259.
- Martínez-Vilalta, J., Piñol, J., 2002. Drought-induced mortality and hydraulic architecture in pine populations of the NE Iberian Peninsula. *For. Ecol. Manage.* 161, 247–256.
- Martínez-Vilalta, J., Piñol, J., Beven, K., 2002. A hydraulic model to predict drought-induced mortality in woody plants: an application to climate change in the Mediterranean. *Ecol. Model.* 155, 127–147.
- Martínez-Vilalta, J., Poyatos, R., Aguadé, D., Retana, J., Mencuccini, M., 2014. A new look at water transport regulation in plants. *New Phytol.*, <http://dx.doi.org/10.1111/nph.12912>
- Maseda, P.H., Fernández, R.J., 2006. Stay wet or else: three ways in which plants can adjust hydraulically to their environment. *J. Exp. Bot.* 57, 3963–3977, <http://dx.doi.org/10.1093/jxb/erl127>
- McDowell, N., Fisher, R., Xu, C., Domec, J., Hölttä, T., Mackay, D., Sperry, J.S., Boutz, A., Dickman, L., Gehres, N., Limousin, J.-M., Macalady, A., Martínez-Vilalta, J., Mencuccini, M., Plaut, J.A., Ogée, J., Pangle, R., Rasse, D., Ryan, M., Sevanto, S., Waring, R., Williams, A., Yepez, E., Pockman, W.T., 2013. Evaluating theories of drought-induced vegetation mortality using a multimodel–experiment framework. *New Phytol.* 200, 304–321.
- McDowell, N., Pockman, W.T., Allen, C.D., Breshears, D.D., Cobb, N., Kolb, T., Plaut, J., Sperry, J., West, A., Williams, D.G., Yepez, E.A., 2008. Mechanisms of plant survival and mortality during drought: why do some plants survive while others succumb to drought? *New Phytol.* 178, 719–739, <http://dx.doi.org/10.1111/j.1469-8137.2008.02436.x>
- McDowell, N.G., Beerling, D.J., Breshears, D.D., Fisher, R.A., Raffa, K.F., Stitt, M., 2011. The interdependence of mechanisms underlying climate-driven vegetation mortality. *Trends Ecol. Evol.* 26, 523–532, <http://dx.doi.org/10.1016/j.tree.2011.06.003>
- McKee, T., Doesken, N., Kleist, J., 1993. The relationship of drought frequency and duration to time scales, in: Eighth Conference on Applied Climatology. pp. 17–22.
- Miralles, D.G., Gash, J.H., Holmes, T.R.H., de Jeu, R.A.M., Dolman, A.J., 2010. Global canopy interception from satellite observations. *J. Geophys. Res.* 115, D16122, <http://dx.doi.org/10.1029/2009JD013530>
- Mouillot, F., Rambal, S., Joffre, R., 2002. Simulating climate change impacts on fire frequency and vegetation dynamics in a Mediterranean-type ecosystem. *Global Change Biol.* 8, 423–437.
- Mouillot, F., Rambal, S., Lavorel, S., 2001. A generic process-based Simulator for mediterranean landscaPes (SIERRA): design and validation exercises. *For. Ecol. Manage.* 147, 75–97, [http://dx.doi.org/10.1016/S0378-1127\(00\)00432-1](http://dx.doi.org/10.1016/S0378-1127(00)00432-1)
- Ninyerola, M., Pons, X., Roure, J.M., 2000. A methodological approach of climatological modelling of air temperature and precipitation through GIS techniques. *Int. J. Climatol.* 20, 1823–1841.
- Oliva, J., Stenlid, J., Martínez-Vilalta, J., 2014. The effect of fungal pathogens on the water and carbon economy of trees: implications for drought-induced mortality. *New Phytol.*
- Pasho, E., Camarero, J.J., de Luis, M., Vicente-Serrano, S.M., 2011. Impacts of drought at different time scales on forest growth across a wide climatic gradient in north-eastern Spain. *Agric. For. Meteorol.* 151, 1800–1811, <http://dx.doi.org/10.1016/j.agrformet.2011.07.018>
- Palmer, W., 1965. Meteorological Drought. *Res. Pap.* 45.
- Pausas, J.G., 2004. Changes in fire and climate in the Eastern Iberian Peninsula (Mediterranean Basin). *Clim. Change* 63, 337–350.
- Pausas, J.G., Fernández-Muñoz, S., 2012. Fire regime changes in the Western Mediterranean Basin: from fuel-limited to drought-driven fire regime. *Clim. Change* 110, 215–226, <http://dx.doi.org/10.1007/s10584-011-0060-6>
- Pausas, J.G., Paula, S., 2012. Fuel shapes the fire-climate relationship: evidence from Mediterranean ecosystems. *Global Ecol. Biogeogr.* 21, 1074–1082.
- Pons, X., Ninyerola, M., 2008. Mapping a topographic global solar radiation model implemented in a GIS and refined with ground data. *Int. J. Climatol.*, 1821–1834, <http://dx.doi.org/10.1002/joc>
- Poyatos, R., Aguadé, D., Galiano, L., Mencuccini, M., Martínez-Vilalta, J., 2013. Drought-induced defoliation and long periods of near-zero gas exchange play a key role in accentuating metabolic decline of Scots pine. *New Phytol.* 200, 388–401.
- Poyatos, R., Llorens, P., Gallart, F., 2005. Transpiration of montane *Pinus sylvestris* L. and *Quercus pubescens* Willd. forest stands measured with sap flow sensors in NE Spain. *Hydrol. Earth Syst. Sci. Discuss.* 2, 1011–1046, <http://dx.doi.org/10.5194/hess-2-1011-2005>
- Poyatos, R., Villagarcía, L., Domingo, F., Piñol, J., Llorens, P., 2007. Modelling evapotranspiration in a Scots pine stand under Mediterranean mountain climate using the GLUE methodology. *Agric. For. Meteorol.* 146, 13–28, <http://dx.doi.org/10.1016/j.agrformet.2007.05.003>
- Prentice, I.C., Sykes, M.T., Cramer, W., 1993. A simulation model for the transient effects of climate change on forest landscapes. *Ecol. Modell.* 65, 51–70, [http://dx.doi.org/10.1016/0304-3800\(93\)90126-D](http://dx.doi.org/10.1016/0304-3800(93)90126-D)
- Rambal, S., Ourcival, J.M., Joffre, R., Mouillot, F., Nouvellon, Y., Reichstein, M., Rocheteau, A., 2003. Drought controls over conductance and assimilation of a Mediterranean evergreen ecosystem: scaling from leaf to canopy. *Global Change Biol.* 9, 1813–1824, <http://dx.doi.org/10.1111/j.1365-2486.2003.00687.x>
- Ritchie, J., 1972. Model for predicting evaporation from a row crop with incomplete cover. *Water Resour. Res.* 8, 1204–1213.
- Ruffault, J., Martin-StPaul, N.K., Duffet, C., Goge, F., Mouillot, F., 2014. Projecting future drought in Mediterranean forests: bias correction of climate models matters! *Theor. Appl. Climatol.* 117, 113–122, <http://dx.doi.org/10.1007/s00704-013-0992-z>
- Ruffault, J., Martin-StPaul, N.K., Rambal, S., Mouillot, F., 2013. Differential regional responses in drought length, intensity and timing to recent climate changes in a Mediterranean forested ecosystem. *Clim. Change* 117, 103–117, <http://dx.doi.org/10.1007/s10584-012-0559-5>
- Ruiz-Benito, P., Lines, E.R., Gómez-Aparicio, L., Zavala, M.A., Coomes, D.A., 2013. Patterns and drivers of tree mortality in iberian forests: climatic effects are modified by competition. *PLoS One* 8, e56843, <http://dx.doi.org/10.1371/journal.pone.0056843>
- Running, S., Coughlan, J., 1988. A general model of forest ecosystem processes for regional applications. I. Hydrologic balance, canopy gas exchange and primary production processes. *Ecol. Modell.* 42, 125–154.

- Saxton, K.E., Rawls, W.J., Romberger, J.S., Papendick, R.I., 1986. *Estimating generalized soil-water characteristics from texture*. Soil Sci. Soc. Am. J. 50, 1031–1036.
- Schenk, H., Jackson, R., 2002. *The global biogeography of roots*. Ecol. Monogr. 72, 311–328.
- Schymanski, S.J., Sivapalan, M., Roderick, M.L., Beringer, J., Hutley, L.B., 2008. An optimality-based model of the coupled soil moisture and root dynamics. Hydrol. Earth Syst. Sci. 12, 913–932, <http://dx.doi.org/10.5194/hess-12-913-2008>
- Sen, P., 1968. *Estimates of the regression coefficient based on Kendall's tau*. J. Am. Stat. Assoc. 63, 1379–1389.
- Sepulcre-Canto, G., Horion, S., Singleton, A., Carrao, H., Vogt, J., 2012. Development of a Combined Drought Indicator to detect agricultural drought in Europe. Nat. Hazard. Earth Syst. Sci. 12, 3519–3531, <http://dx.doi.org/10.5194/nhess-12-3519-2012>
- Sheffield, J., Wood, E.F., 2008. Global trends and variability in soil moisture and drought characteristics, 1950–2000, from observation-driven simulations of the terrestrial hydrologic cycle. J. Clim. 21, 432–458, <http://dx.doi.org/10.1175/2007JCLI1822.1>
- Sitch, S., Smith, B., Prentice, I.C., Arneth, A., Bondeau, A., Cramer, W., Kaplan, J.O., Lewis, S., Lucht, W., Sykes, M.T., Thonicker, K., Venevsky, S., 2003. Evaluation of ecosystem dynamics, plant geography and terrestrial carbon cycling in the LPJ dynamic global vegetation model. Global Change Biol. 9, 161–185, <http://dx.doi.org/10.1046/j.1365-2486.2003.00569.x>
- Sperry, J.S., Adler, F.R., Campbell, G.S., Cornstock, J.P., 1998. *Limitation of plant water use by rhizosphere and xylem conductance: results from a model*. Plant. Cell Environ. 21, 347–359.
- Stolfi, R., Thurler, Á., Oliveira, O., Bacchi, S., Reichardt, K., 2011. *Method to estimate soil macroporosity and microporosity based on sand content and bulk density*. Rev. Bras. Ciencias do Solo 35, 447–459.
- Sus, O., Poyatos, R., Barba, J., Carvalhais, N., Llorens, P., Williams, M., Vilalta, J.M., 2014. Time variable hydraulic parameters improve the performance of a mechanistic stand transpiration model. A case study of Mediterranean Scots pine sap flow data assimilation. Agric. For. Meteorol. 198–199, 168–180, <http://dx.doi.org/10.1016/j.agrformet.2014.08.009>
- Tague, C.L., McDowell, N.G., Allen, C.D., 2013. An integrated model of environmental effects on growth, carbohydrate balance, and mortality of Pinus ponderosa forests in the southern Rocky Mountains. PLoS One, 8, <http://dx.doi.org/10.1371/journal.pone.0080286>
- Tesfa, T.K., Tarboton, D.G., Chandler, D.G., McNamara, J.P., 2009. Modeling soil depth from topographic and land cover attributes. Water Resour. Res. 45, W10438, <http://dx.doi.org/10.1029/2008WR007474>
- Vayreda, J., Martínez-Vilalta, J., Gracia, M., Retana, J., 2012. Recent climate changes interact with stand structure and management to determine changes in tree carbon stocks in Spanish forests. Global Change Biol. 18, 1028–1041, <http://dx.doi.org/10.1111/j.1365-2486.2011.02606.x>
- Vicente-Serrano, S.M., Beguería, S., López-Moreno, J.I., 2010. a multiscalar drought index sensitive to global warming: the standardized precipitation evapotranspiration index. J. Clim. 23, 1696–1718, <http://dx.doi.org/10.1175/2009JCLI2909.1>
- Vilà-Cabrera, A., Martínez-Vilalta, J., Vayreda, J., Retana, J., 2011. *Structural and climatic determinants of demographic rates of Scots pine forests across the Iberian Peninsula*. Ecol. Appl. 21, 1162–1172.
- Villaescusa, R., Díaz, R., 1998. *Segundo inventario forestal nacional (1986–1996)*. Ministerio de Medio Ambiente, ICONA, Madrid.
- Villanueva, J.A., 2004. *Tercer inventario forestal nacional (1997–2007)*. Ministerio de Medio Ambiente y Medio Rural, ICONA, Madrid.
- Weisseiner, C.J., Boschetti, M., Böttcher, K., Carrara, P., Bordogna, G., Brivio, P.A., 2011. Spatial explicit assessment of rural land abandonment in the Mediterranean area. Global Planet Change 79, 20–36, <http://dx.doi.org/10.1016/j.gloplacha.2011.07.009>
- Weltzin, J.F., Loik, M.E., Schwinning, S., Williams, D.G., Fay, P.A., Haddad, B.M., Harte, J., Huxman, T.E., Knapp, A.K., Lin, G., Pockman, W.T., Shaw, M.R., Small, E.E., Smith, M.D., Smith, S.D., Tissue, D.T., Zak, J.C., 2003. Assessing the response of terrestrial ecosystems to potential changes in precipitation. Bioscience 53, 941–952. doi:10.1641/0006-3568(2003)053[0941:ATROTE]2.0.CO;2.
- Zavala, M.A., Bravo de la Parra, R., 2005. A mechanistic model of tree competition and facilitation for Mediterranean forests: Scaling from leaf physiology to stand dynamics. Ecol. Modell. 188, 76–92, <http://dx.doi.org/10.1016/j.ecolmodel.2005.05.006>
- Zheng, D., Hunt Jr, E.R., Running, S.W., 1996. *Comparison of available soil water capacity estimated from topography and soil series information*. Landsc. Ecol. 11, 3–14.